PRIFYSGOL BANGOR / BANGOR UNIVERSITY

PRIFYSGOL
BANGOR
UNIVERSITY

Co(II)-doped hybrid Zn(II) tetraborate complexes, [ZnxCo(1-x)(1,3-dap)B4O7] (1,3-dap = 1,3-diaminopropane): BET analysis and N2/H2O/D2O adsorption studies

Liu, Lei; Pan, Chun-Yang; He, yong ; Zhong, Li-Juan; Beckett, Michael

Dalton Transactions

DOI:
10.1039/D4DT00117F

E-pub ahead of print: 05/02/2024

Peer reviewed version

Cyswllt i'r cyhoeddiad / Link to publication

Dyfyniad o'r fersiwn a gyhoeddwyd / Citation for published version (APA):
Liu, L., Pan, C.-Y., He, Y., Zhong, L.-J., & Beckett, M. (2024). Co(II)-doped hybrid Zn(II) tetraborate complexes, [ZnxCo(1-x)(1,3-dap)B4O7] (1,3-dap = 1,3-diaminopropane): BET analysis and N2/H2O/D2O adsorption studies. *Dalton Transactions*, *53*(10), 4637-4642. Advance online publication. https://doi.org/10.1039/D4DT00117F

Hawliau Cyffredinol / General rights
Copyright and moral rights for the publications made accessible in the public portal are retained by the authors and/or other copyright owners and it is a condition of accessing publications that users recognise and abide by the legal requirements associated with these rights.

• Users may download and print one copy of any publication from the public portal for the purpose of private study or research.
• You may not further distribute the material or use it for any profit-making activity or commercial gain
• You may freely distribute the URL identifying the publication in the public portal ?

Take down policy
If you believe that this document breaches copyright please contact us providing details, and we will remove access to the work immediately and investigate your claim.

09. Mar. 2025

ARTICLE

$Co^{(II)}$-doped hybrid $Zn^{(II)}$ tetraborate complexes, $[Zn_xCo_{(1-x)}(1,3\text{-dap})B_4O_7]$ (1,3-dap = 1,3-diaminopropane): BET analysis and $N_2/H_2O/D_2O$ adsorption studies†

Received 00th January 20xx,
Accepted 00th January 20xx

DOI: 10.1039/x0xx00000x

Lei Liu,[a] Chun-Yang Pan,*[a] Yong He,[a] Li-Juan Zhong,[a] Michael A. Beckett [b]

A series of mono/bimetallic isostructural hybrid tetraborates of general formula $[Zn_xCo_{(1-x)}(1,3\text{-dap})B_4O_7]$ have been prepared by a solvothermal method. Their adsorption/desorption curves for H_2O and D_2O demonstrate that these materials have a stronger affinity for H_2O than for D_2O and enrich the D_2O content of D_2O/H_2O mixtures.

Introduction

Solid-state oxidoborate materials have attracted considerable research interest due to the variety of their structures and their potential applications in catalysis, ion exchange and nonlinear optical properties.[1-6] Recent research has also focused on the structures and properties of novel hybrid (inorganic/organic) oxidoborates synthesized using organic templates.[7-15] There is extensive and well-known research investigating porous materials such as silicates and MOFs.[16-20] Porous materials have been used to sieve molecules of specific size and have found applications as gas separation (VOCs), desiccants (water adsorption), catalysts in petrochemical refineries, and as ion-exchange (water softening) materials. Oxidoborates have similar structures to MOFs and therefore these hybrid materials have potential as tunable porous host structures with unique sieve-like adsorption properties.[21-28] These properties of such compounds are currently being explored in our laboratories.[29]

Adsorption and separation of gases by MOFs have also made a great contribution to modern industries, *e.g.* the absorption and degradation of CO_2 for contemporary environmental protection the separation of ethylene/ethane in high-purity ethylene production, [30,31] ^2H and ^1H isotope separation,[32] and Xe and Kr rare gas separation.[33] Intermediate size molecular sieves have also been developed with "open hole" behavior to separate high purity styrene from mixtures of larger molecules such as ethylbenzene, styrene, toluene and benzene and flexible porous MOF materials with 'gated' memories or 'shape specific' memories have also been synthesized and used in sieve-type adsorption separations.[34-37]

Heavy water (D_2O) is an important chemical and is extensively used in the field of nuclear energy. Separation of D_2O from light water (H_2O) is very difficult due to their similar physical and chemical properties. Currently the separation of heavy water from H_2O is achieved through costly, energy intensive, chemical exchange (e.g. the Girdler sulfide process), distillation or electrolysis.[38-39] Gu *et al*. have reported two cases of copper-based MOF materials with a cage structure.[40] The small-diameter windows on them can be opened at the given temperature to achieve H_2O/D_2O separation. Their work has provided a feasible new solution for the separation of D_2O from H_2O by using porous materials. Though porous materials are widely used for selective adsorption of gases, there are relatively few reports on the purification of liquids with small size, especially D_2O.[41-43]

In this manuscript we describe the synthesis of a series of mixed metal hybrid oxidoborates (Figure 1) with the intention of exploring their ability to selectively sieve small molecules such as D_2O and H_2O. N_2 BET adsorption analysis has been used to confirm that the pore size and the pore distribution of the hybrid mixed metal oxidoborates. These materials are tunable and properties are dependent on the metal molar ratios. ^1H NMR has been used to demonstrate selective adsorption of H_2O by these oxidoborates from D_2O/H_2O mixtures.

[a] *School of Light Industry and Chemical Engineering, Guangdong University of Technology, Guangzhou 510006 (P.R. China)*
E-mail: panchuny@gdut.edu.cn
[b] *School of Natural Sciences, Bangor University, Gwynedd, LL57 2UW, UK.*

† Footnotes relating to the title and/or authors should appear here.
Electronic Supplementary Information (ESI) available: FT-IR spectra and ^1H NMR spectroscopy. See DOI: 10.1039/x0xx00000x

Please do not adjust margins

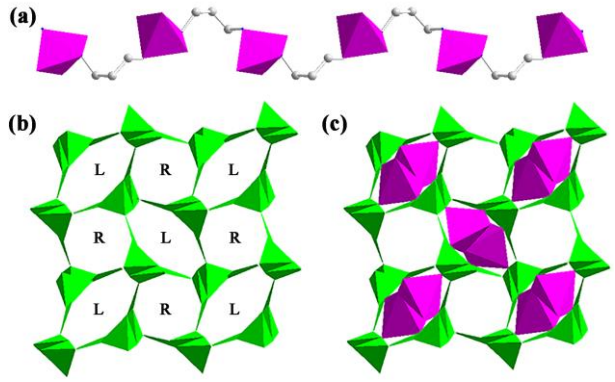

Figure 1. (a) $Zn_xCo_{1-x}O_3N_2$ trigonal bipyramids linked by 1,3-dap molecules to give rise to a 1D Zn_xCo_{1-x} (1,3-dap)O_3 chain; (b) a view of the 8 M helical rings of Zn_xCo_{1-x} (1,3-dap)O_4O_7 in order of R- and L-handed helix, R: right, L: left; (c) $Zn_xCo_{1-x}O_3N_2$ trigonal bipyramids filled 8 M L-helical channels. Color codes: C atom is gray, $Zn_xCo_{1-x}O_3N_2$ trigonal bipyramid is purple, BO_4 tetrahedron and BO_3 triangle are green.

Experimental section

Synthesis of [Zn(1,3-dap)B_4O_7](1)

A mixture of $Zn(OH)_2$ (0.099 g, 1 mmol), H_3BO_3 (0.496 g, 8 mmol), and a solvent comprised of 1,3-propylenediamine (1,3-dap) (1.0 mL), ethanol (2.0 mL), and pyridine (2.0 mL) was stirred for 2 h. The mixture was sealed in a 25 mL Teflon-lined high-pressure steel reactor and then heated in an oven at 453 K. After 9 days the steel reactor was taken out and cooled to room temperature, bulk crystals of **1** (0.283 g, 48% yield, based on H_3BO_3) were obtained by filtration, washed with absolute ethanol, and dried in air at room temperature [29]. Repeat experiments generated material for the H_2O/D_2O adsorption experiments.

Synthesis of [$Zn_xCo_{(1-x)}$1,3-dap)B_4O_7] (2-5)

Compounds **2**-**5** were prepared as purple crystals by a similar method as used in the synthesis of **1** except that $Zn(OH)_2$ (0.099 g, 1 mmol) was replaced by a mixture of $Zn(OH)_2$ and $Co(OH)_2$ (to a total of 1 mmol). Zn:Co molar ratios of 9:1, 7:3, 5:5, 3:7, was used for synthesis of **2**-**5**, respectively. The masses obtained for **2**-**5** and their yields (based on H_3BO_3) were as follows: **2**, 0.247 g, 42%; **3**, 0.204 g, 35%; **4**, 0.169 g, 29%; **5**, 0.139 g, 24%. ICP determined Zn/Co ratios for **2**-**5** were of 9.43:1 (**2**), 2.73:1 (**3**), 1.1:1 (**4**), 0.23:1 (**5**) respectively, giving experimentally determined stoichiometries of [$Zn_{0.90}Co_{0.10}$(1,3-dap)B_4O_7] (**2**), [$Zn_{0.73}Co_{0.27}$(1,3-dap)B_4O_7] (**3**), [$Zn_{0.52}Co_{0.48}$(1,3-dap)B_4O_7] (**4**) and [$Zn_{0.19}Co_{0.81}$(1,3-dap)B_4O_7] (**5**).

Synthesis of [Co(1,3-dap)B_4O_7] (6)

Compound **2** was obtained by procedure similar to that for **1**, except that the $Zn(OH)_2$ (0.099 g, 1mmol) was replaced by $Co(OH)_2$ (0.0929 g, 1 mmol). Compound **6** was obtained as a purple solid (0.121 g, 21% yield, based on H_3BO_3).

Thermal drying/activation of 1-6

The resulting **1** (1.3489 g), **2** (0.9561 g), **3** (0.6417 g), **4** (1.2210 g), **5** (0.1229 g), and **6** (0.2031 g) were heated to 573K in muffle furnace for one hour (temperature setting T_1 = 298K, T_2 = 573K, T_3 = 573 K, T_4 = 298K; Time C_1 = 60 min, C_2 = 60 min, C_3 = 60 min). The masses of **1** - **6** after thermal activation were 1.3403 g, 0.9174 g, 0.5986 g, 1.1671 g, 0.1060g, 0.2014 g respectively.

BET analysis (N_2)

The porous structure of **1**, **4** and **6** was characterized by the N_2 adsorption–desorption isotherms, which were measured at 77 K using a chemisorption–physisorption analyzer (Autosorb-1-C, Quantachrome, Boynton Beach, FL, USA) after the samples had been previously degassed at 573 K for 1.0 h Pore sizes were evaluated from the N_2 desorption isothermal using the Barrett–Joyner–Halenda (BJH) method.[57] Size distribution data were obtained and BET analysis gave the total pore volumes of **1**, **4** and **6** to be 0.009481, 0.01194, 0.0197 m^3/g respectively.[44]

D_2O/H_2O adsorption isotherm

D_2O/H_2O adsorption isotherms were measured by an Autosorb-iQ (Quantachrome Instru-ments US) with the mass inaccuracy is ±0.001 g. The instrument was automatically operated to precisely control the vapor pressure (1–95% RH) and temperature (298 K). Prior to adsorption experiments, samples were completely dehydrated at 573 K for 8 h to a constant weight.

Selective D_2O/H_2O adsorption experiments as followed by ^1H NMR

Stock 50:50 (v/v) and 90:10 (v/v) D_2O/H_2O mixtures (100ml) was prepared and used with a 5 mL Pasteur pipette as solid-liquid absorption apparatus. In separate experiments 1.0g of the hybrid borates **1**-**6** were placed on top of *ca.* 0.07 g of dried cotton wool and 1.00 mL of a D_2O/H_2O solution was added, with the pipette clamped at the lower end. After allowing 2 hours for adsorption, the clamp was opened and the D_2O/H_2O mixtures were collected for analysis by ^1H NMR spectroscopy.

^1H NMR adsorption study

^1H spectra were recorded on a Bruker Avance III 400 MHz Superconducting Fourier system in 0.5mm OD sample tubes containing 500μL of the samples obtained from the absorption experiments and 50μL of $(CH_3)_2SO$ (DMSO) as an internal standard. A 'blank' 500μL stock D_2O/H_2O mixture containing 250μL of both D_2O and H_2O and 50μL DMSO was also prepared. Spectra all showed 2 peaks (both singlets) at d 4.70 (H_2O) and d 2.63 (DMSO) and their relative intensities (H_2O:DMSO) were determined by integration as follows: From the 50:50 D_2O/H_2O stock: Blank, 6.57:1; 1, 6.53:1; 2, 6.31:1, 3, 6.23:1; 4, 6.08:1; 5, 5.63:1, 6, 5.50:1. These data were normalized relative to the 'blank'. From the 90:10 D_2O/H_2O stock: Blank, 1.34:1; 1, 1.34:1; 2, 1.32:1, 3, 1.30:1; 4, 1.30:1; 5, 1.29:1, 6, 1.26:1. These data were also normalized relative to the' blank'.

This journal is © The Royal Society of Chemistry 20xx

Please do not adjust margins

Please do not adjust margins

Results and discussion

We have previously reported the synthesis and of the hybrid tetraborate (2-) complex [Zn(1,3-dap)B_4O_7] (**1**),[29] and we have used the same methodology to prepare a series of mixed metal $Co^{(II)}/Zn^{(II)}$ [$Zn_xCo_{(1-x)}$(1,3-dap)B_4O_7] (**2**-**5**) derivatives and [Co(1,3-dap)B_4O_7] (**6**). Compound **6** has been previously reported by Yang and co-workers.[44] The powder-XRD pattern of **6**, as prepared by our method, is identical with that reported in the literature.[44] TGA/DSC plots of samples **1** and **6** were also consistent with the literature.[29,44] Compounds **1** and **6** are isomorphic and their structures have trigonal bipyramidal configurations about the metal centers with the metal coordinated by two different 1,3-dap ligands (Figure 1). The 1,3-dap ligands bridge two metal centers and form coordination polymer chains. The heptaoxidotetraborate network has consists of a FBB of 4 *i.e.* (4-1):(2T + 2D) condensed into a zeolitic type framework with helical channels.[21-23, 28]

The p-XRD pattern (Figure 2) presents well-defined peaks, and the hybrid tetraborates with different proportions of Zn and

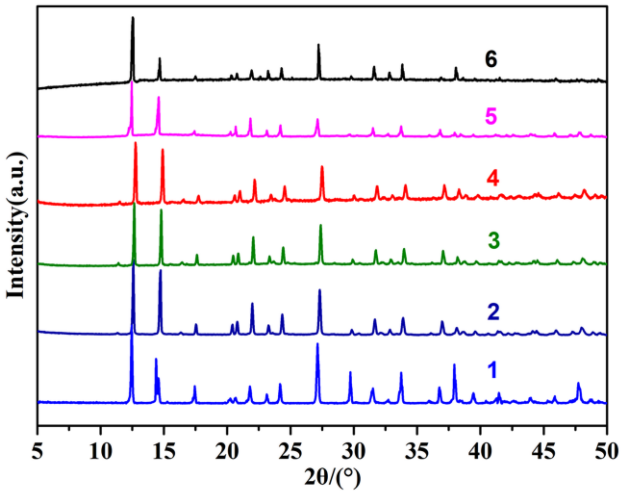

Figure 2. P-XRD patterns of **1**-**6**.

Co are consistent with the characteristic peaks of **1** which confirm their purity. The difference in strength is caused by the different anisotropy of the crystal planes and the inconsistent preferential orientation of the crystal. Inductively coupled plasma (ICP) (Zn/Co) analysis was used to experimentally determine the stoichiometry of the mixed metal tetraborates as [$Zn_{0.90}Co_{0.10}$(1,3-dap)B_4O_7] (**2**), [$Zn_{0.73}Co_{0.27}$(1,3-dap)B_4O_7] (**3**), [$Zn_{0.52}Co_{0.48}$(1,3-dap)B_4O_7] (**4**) and [$Zn_{0.19}Co_{0.81}$(1,3-dap)B_4O_7] (**5**). These experimentally determined values were consistent with the stoichiometry expected from the Zn/Co ratios used in the synthetic procedures. Since **1**, **4** and **6** are crystallographically isostructural their IR spectra are all very similar (Figure S1).

To confirm that **2**-**5** were doped homogeneous oxidoborates rather than a 'simple mixtures' of **1** and **6** a detailed micron scale surface scanning by high-angle annular dark field – scanning transmission electron microscopy (HAADF-STEM)/Energy-dispersive X-ray Spectroscopy (EDAX) experiment was carried out on a **4**, as a representative example. These scans for **4** are shown in Figure 3. Each of the elements present in **4** are evenly distributed confirming that **4** was successfully prepared as a doped material and we infer from this that **2**, **3** and **5** prepared by similar methods, should also be doped materials.

Fig 3 here

Low-pressure H_2O and D_2O adsorption isotherms (298 K) were obtained for **1**, **4** and **6**. The H_2O adsorption/desorption curves for **1**, **4** and **6** are shown in Figure 4(a) where it can be seen that the $Co^{(II)}$-borate **6** can adsorb approximately 3-times more H_2O than **1**, the $Zn^{(II)}$-borate, with adsorption properties of the mixed metal $Co^{(II)}/Zn^{(II)}$-borate **4** being in between these two extremes. A similar set of curves was observed for D_2O adsorption (Figure 4(b)), but adsorption values were lower, when compared to H_2O, for all three materials. This led us to

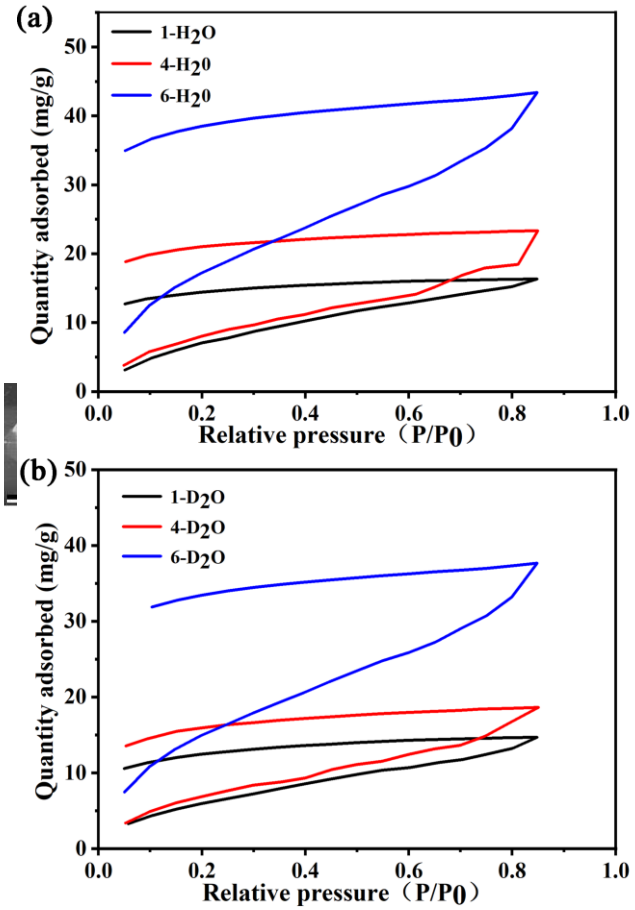

Figure 4. (a) H_2O adsorption-desorption curves for **1**, **4** and **6**, (b) D_2O adsorption-desorption curves for **1**, **4** and **6**

believe that these hybrid borates might have a potential application as adsorbents for separating or enriching D_2O/H_2O mixtures.

This hypothesis was explored by ^1H NMR spectroscopy (Figure S2). In an initial series of experiments the hybrid borates **1**-**6** were separately allowed to adsorb synthetic H_2O/D_2O (50:50, by vol.) mixtures and the residual H_2O/D_2O was examined by ^1H NMR using DMSO as a quantitative internal standard. Results are presented in Figure 5(a). Spectra are in Figure S2. The relative intensity of the H_2O signals decrease as

Please do not adjust margins

the proportion of $Co^{(II)}$ in the hybrid borate increase; **6** has the lowest proportion of H_2O present in the residual H_2O/D_2O mixture, indicating that **6** preferentially adsorbs H_2O over D_2O and that residual water is effectively D_2O enriched. Quantitatively, the ^1H NMR data indicate that with **6** as the adsorbent the H_2O concentration in the residual D_2O/H_2O mixture drops by 16% compared to the blank, leaving an enriched D_2O:H_2O composition of 58:42. Similar results were obtained from synthetic H_2O/D_2O (10:90 by vol.) (Figure 5(b)) where the concentration of residual H_2O in the mixture decreased on progression from **1**-**6** confirming that **6** had the greatest affinity for H_2O of the hybrid borates, with a drop of 6% compared to the blank. Quantitatively, this small percentage drop would indicate a real, but minimal, D_2O enrichment of the mixture leaving a residual D_2O:H_2O composition of 90.6:9.4.

Fig 5 here

Compounds **1**, **4** and **6** were selected as representative examples and nitrogen adsorption and desorption at 77K was used to characterize the porosity and the mesopore size of these materials. BET analysis using nitrogen adsorption desorption isotherms (Figure 6) indicates the surface areas of **1**, **4** and **6** are 2.744, 8.807, 14.583 m^2/g,[45-47] and total pore volumes of 0.009481, 0.01194, 0.0197 m^3/g, respectively. These values are similar to those reported for a microporous functional polyurethane porous organic framework (POF),[48] but generally higher than those observed in non-metal cation oxidoborates.[49,50]

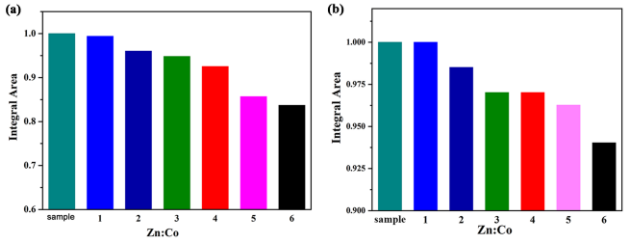

Figure 5. ^1H NMR: the relative integral area of H_2O, relative to an internal standard, after adsorption of synthetic D_2O/H_2O mixtures by the hybrid borates **1-6**. (a) D_2O:H_2O, 50:50 by vol., (b) D_2O:H_2O, 90:10 by vol.

FIG 6 here.

The pore size distribution results are shown in Figure 7. Samples **1**, **4** and **6** have similar pore size distribution, but the introduction of cobalt into **4** and **6** shifts the pore size distribution plots to slightly higher values. This may be explained since $Co^{(II)}$ has a larger ionic radius/volume than $Zn^{(II)}$, and therefore the size and the number of pores can be fine-tuned by adjusting the proportion of $Co^{(II)}$ in the hybrid borate. The plots in Figure 7 indicate that all three materials can be classified as microporous with the majority of pores <5 nm diameter and very few pores at a diameter of >10 nm. The hysteresis loops correspond to type I, type II with H4, respectively.[51] The overlap of adsorption and desorption curves at $P/P_0 < 0.1$ is related to the filling of micropores. H4 loops are known to exist in some zeolites and micro-mesoporous carbons.

As noted above the doping of $Co^{(II)}$ into the $Zn^{(II)}$ borate lattice increase pore size and distribution and this may have led to the difference in the diffusion rate of H_2O and D_2O in **6**. It seems very likely that H-bonding/D-bonding is involved in the H_2O/D_2O adsorption interactions with the oxidoborate adsorbent since

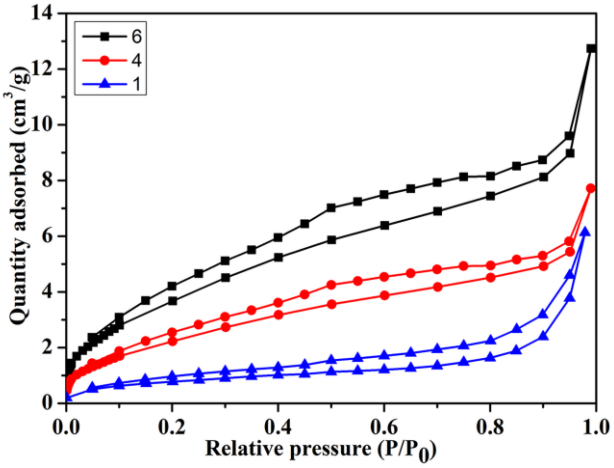

Figure 6. Nitrogen adsorption and desorption isotherms of **1**, **4**, and **6** at 77 K.

such interactions are of primary importance in MOFs and zeolites with water.[52-58] At present we can only speculate as to why **6** prefers to adsorb H_2O other D_2O but in these related systems hydrophilicity/hydrophobicity properties of the framework and the relative strengths of water-water and water-framework interactions are important.[54-57] The 1,3-diaminopropane linkers are likely to generate hydrophobic

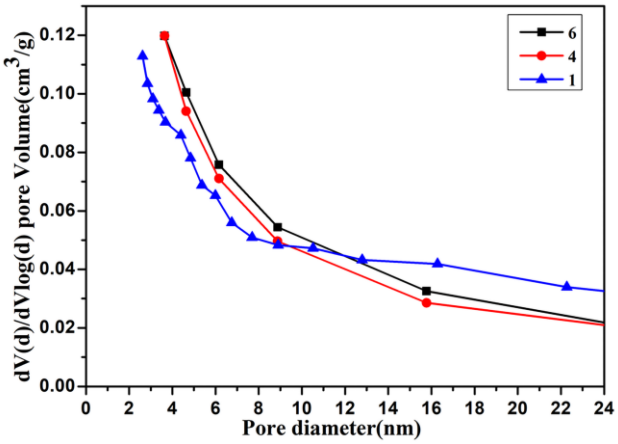

Figure 7. Aperture distribution of **1**, **4** and **6**

regions within the otherwise hydrophilic oxidoborate framework and as such the adsorbent can offer differing H-bonding/D-bonding opportunities to the D_2O/H_2O adsorbates.

Conclusion

This work demonstrates the ability of thermally activated microporous hybrid $[Zn_xCo_{(1-x)}(1,3\text{-dap})B_4O_7]$ materials to adsorb small molecules such as water. Their

This journal is © The Royal Society of Chemistry 20xx

Please do not adjust margins

Please do not adjust margins

adsorption/desorption curves for H_2O and D_2O demonstrate that these materials have a stronger affinity for H_2O than for D_2O. Adsorption experiments involving adsorption from a 1:1 and 9:1 (both by volume) mixtures of D_2O/H_2O using these adsorbents were performed and quantitative ^1H NMR analysis confirmed that the residual water was enriched in D_2O. Adsorbent properties of the bimetallic (doped) hybrid oxidoborates were regulated by the value of x in $[Zn_xCo_{(1-x)}(1,3\text{-dap})B_4O_7]$ demonstrating that fine-tuning of hybrid oxidoborate materials, in this and other potential applications, is feasible.

Conflicts of interest

There are no conflicts to declare.

Acknowledgements

This work was supported by the National Natural Science Foundation of China (No. 21671044).

Notes and references

1 E. R. Wang, J. H. Huang, S. J. Yu, Y. Z. Lan, J. Cheng, G. Y. Yang, *Inorg. Chem.*, 2017**, 56**, 6780-6783.
2 G. Q. Shi, Y. Wang, F. F. Zhang, B. B. Zhang, Z. H. Yang, X. L. Hou, S. L. Pan, K. R. Poeppelmeier, *J. Am. Chem. Soc.*, 2017**, 139**, 10645-10648.
3 F. Lin, Y. P. Dong, J. Y. Peng, L. P. Wang, W. Li, *Phase Transitions,* 2016**, 89**, 558-567.
4 C. Wu, L. H. Li, J. L. Song, G. Y. Yang, M. G. Humphrey, C. Zhang, *Inorg. Chem.,* 2017**, 56**, 1340-1348.
5 E. Kaewnuam, N. Wantana, H. J. Kim, J. Kaewkhao, *J. Non. Cryst. Solid,* 2017**, 464**, 96-103.
6 A. M. Smith, L. Trotochaud, M. S. Burke, S. W. Boettcher, *Chem. Commun.,* 2015**, 51**, 5261-5263.
7 C. A. Chen, G. Y. Yang, *CrystEngComm,* 2022, **24**, 1203-1210.
8 Q. Han, J. C. Liu, Y. Wen, L. J. Chen, J. Zhao, G. Y. Yang, *Inorg. Chem.,* 2017**, 56**, 7257-7269.
9 W. H. Fang, G. Y. Yang, *Inorg. Chem.,* 2014**, 53**, 5631-5636.
10 S. T. Zheng, J. Zhang, X. X. Li, W. H. Fang, G. Y. Yang, *J. Am. Chem. Soc.,* 2010**, 132**, 15102-15103.
11 X. Li, Y. Wang, R. Wang, C. Cui, C. Tian, G. Y. Yang, *Angew. Chem. Int. Edit.,* 2016**, 55**, 6462-6466.
12 W. H. Fang, L. Zhang, J. Zhang, G. Y. Yang, *Chem. Commun.,* 2016**, 52**, 1455-1457.
13 W. H. Fang, L. Zhang, J. Zhang, G. Y. Yang, *Chem. Commun.,* 2015**, 51**, 17174-17177.
14 J. H. Wang, Q. Wei, J. W. Cheng, H. He, B. F. Yang, G. Y. Yang, *Chem. Commun.,* 2015**, 51**, 5066-5068.
15 L. Cheng, G. Y. Yang, *Chem. Commun.,* 2014**, 50**, 344-346.
16 R. M. Barrer, *Zeolites,* 1981**, 1**, 130-140.
17 E. J. P. Feijen, J. A. Martens, P. A. Jacobs, *Stud. Surf. Sci. Catal.,* 1994, **84**, 3-21.
18 T. Ennaert, J. V. Aelst, J. Dijkmans, R. D. Clercq, W. Schutyser, M. Dusselier, D. Verboekend, B. F. Sels, *Chem. Soc. Rev.*, 2016, **45**, 584-611.
19 J. Y. Li, A. Corma, J. H. Yu, *Chem. Soc. Rev.,* 2015, **44**, 7112-7127.
20 M. Dusselier, M. E. Davis, *Chem Rev.,* 2018, **118**, 5265-5329.
21 C. L. Christ, J. R. Clark, *Phys. Chem. Minerals,* 1977, **2**, 59-87.
22 G. Heller, *Top. In Curr. Chem.,* 1986, **131**, 39-98.
23 J. D. Grice, P. C. Burns, F. C. Hawthorne, *Canad. Min.,* 1999, **37**, 731-762.
24 D. M. Schubert, *Struct. Bond.,* 2003, **105**, 1-40.
25 E. L. Belokoneva, *Crystallogr. Rev.,* 2005, **11**, 151-198.
26 M. A. Beckett, *Coord. Chem. Rev.,* 2016, **323**, 2-14.
27 M. A. Altahan, M. A. Beckett, S. J. Coles, P. N. Norton, *J. Clust. Sci.,* 2018, **29**, 1337-1343.
28 S. S. Xin, M. H. Zhou, M. A. Beckett, C. Y. Pan, *Molecules,* 2021, **26**, 3815.
29 C. Y. Pan, L. J. Zhong, F. H. Zhao, H. M. Yang, J. Zhou, *Chem. Commun.,* 2015, **51**, 753-756.
30 P. G. Boyd, A. Chidambaram, E. García-Díez, C. P. Ireland, T. D. Daff, R. Bounds, A. Gładysiak, P. Schouwink, S. M. Moosavi, M. M. Maroto-Valer, J. A. Reimer, J. A. R. Navarro, T. K. Woo, S. Garcia, K. C. Stylianou, B. Smit, *Nature,* 2019, **576**, 253-256.
31 L. B. Li, R. H. Lin, R. Krishna, H. Li, S. Xiang, H. Wu, J. P. Li, W. Zhou, B. L. Chen, *Science,* 2018, **362**, 443.
32 L. Zhang, S. Jee, J. Park, M. Jung, D. Wallacher, A. Franz, W. Lee, M. Yoon, K. Choi, M. Hirscher, H. Oh, *J. Am. Chem. Soc.,* 2019, **141**, 19850-19858.
33 Q. J. Wang, T. Ke, L. F. Yang, Z. Q. Zhang, X. L. Cui, Z. B. Bao, Q. L. Ren, Q. W. Yang, H. B. Xing, *Angew. Chem. Int. Edit.,* 2020, **59**, 3423-3428.
34 Y. Wang, N. Huang, X. Zhang, H. He, R. Huang, Z. Ye, Y. Li, D. Zhou, P. Liao, X. Chen, J. Zhang, *Angewandte Chemie International Edition,* 2019, **58**, 7692-7696.
35 P. Liao, N. Y. Huang, W. X. Zhang, J. P. Zhang, X. M. Chen, *Science,* 2017, **356**, 1193.
36 X. Yang, H. L. Zhou, C. T. He, Z. W. Mo, J. W. Ye, X. M. Chen, J. P. Zhang, *Research,* 2019, **1**, 9.
37 X. W. Zhang, D. D. Zhou, J. P. Zhang, *Chem,* 2021, **7**, 1006-1019.
38 H. K. Rae, *ACS Symposium Series,* 1978, 68, Ch. **1**, 1-26.
39 V. D. Trenin, S. N. Chernoby, I. A. Alekseev, G. A. Sukhorukova, I. A. Baranov, O. A. Fedorchenko, S. D. Bondarenko, V. V. Uborski, *Fusion Technol.*, 1995, **28**, 1579-1584.
40 Y. Su, K. Otake, J. J. Zheng, S. Horike, S. Kitagawa, C. Gu, *Nature*, 2022, **611**, 289-294.
41 A. King, F. W. James, C. G. Lawson, H. V. A. Briscoe, *J. Chem. Soc.,* 1935, **1**, 1545-1549.
42 I. A Bardina, O. S. Zhukova, N. V. Kovaleva, S. N. Lanin, *Russ. J. Phys. Chem. A*, 2007, **81**, 1525–1531.
43 Y. One, R. Futamura, Y. Hatton, T. Sakai, K. Kaneko, *J. Colloid Interf. Sci.,* 2017, **508**, 14-17.
44 S. C. Zhi, Y. L. Wang, L. Sun, J. W. Cheng, G. Y. Yang, *Inorg. Chem.,* 2018, **57**, 1350-1355.
45 S. Brunauer, P. H. Emmett, E. Teller, *J. Amer. Chem. Soc.*, 1938, **60**, 309-319.
46 G. Fagerlund, *Matériaux et Construction,* 1973, **6**, 239-245.
47 P. Sinha, A. Datar, C. Jeong, X. P. Deng, Y. G. Chung, L. C. Lin, *J. Phys. Chem. C,* 2019, **123**, 20195-20209.
48 S. K. Dey, N. S. Amadeu, C. Janiak, *Chem. Commun.,* 2016, **52**, 7834.-7837.
49 M. A. Beckett, P. N. Horton, M. B. Hursthouse, D.A. Knox, J. L. Timmis, *Dalton Trans.,* 2010, **39**, 3944-3951.
50 M. A. Beckett, P. N. Horton, M. B. Hursthouse, D.A. Knox, J. L. Timmis, K. S. Varma, *Dalton Trans.,* 2012, **41**, 4396-4403.
51 K. S. W. Sing, D. H. Everett, R. A. W. Hawl, L. Moscou, R. A. Pierotti, J. Rouquerol, T. Siemieniewska, *Pure Appl. Chem.,* 1985, **57**,603-619.
52 S. Scheiner, M. Cuma, *J. Am. Chem. Soc.,* 1996, **118**, 1511-1521.
53 T. Clark, J. Heske, T. D. Kuhne, *ChemPhysChem,* 2019, **20**, 2461-2465.
54 A. J. Rieth, K. M. Hunter, M. Dinca, F. Paesani, *Nat. Commun.,* 2019, **10**, 4771.

Please do not adjust margins

Please do not adjust margins

55 K. M. Hunter, J. C. Wagner, M. Kalaj, S.M. Cohen, W. Xiong, F. Paesani, *J. Phys. Chem. C,* 2021, **125**, 12451−12460.
56 J. C. Wagner, K. M. Hunter, F. Paesani, W. Xiong, *J. Am. Chem. Soc.,* 2021, **143**, 21189–21194.
57 D. T. Bregante, M. C. Chan, J. J. Tan, E. Z. Ayla, C. P. Nicholas, D. Shukla, D. W. Flaherty, *Nature Catalysis*, 2021, **4**, 797–808.
58 E. P. Barrett, L. G. Joyner, P. P. Halenda, *J. Amer. Chem. Soc.*, 1951, **73**, 373-380.

 This journal is © The Royal Society of Chemistry 20xx

Please do not adjust margins